

Detection accuracy of proximal caries by phosphor plate and cone-beam computerized tomography images scanned with different resolutions

Jun-Ge Cheng · Zhi-Ling Zhang · Xiao-Yan Wang ·
Zu-Yan Zhang · Xu-Chen Ma · Gang Li

Received: 20 January 2011 / Accepted: 19 July 2011 / Published online: 30 July 2011
© Springer-Verlag 2011

Abstract This study was carried out to assess whether the spatial resolution has an impact on the detection accuracy of proximal caries in flat panel CBCT (cone beam computerized tomography) images and if the detection accuracy can be improved by flat panel CBCT images scanned with high spatial resolution when compared to digital intraoral images. The CBCT test images of 45 non-restored human permanent teeth were respectively scanned with the ProMax 3D and the DCT Pro scanners at different resolutions. Digital images were obtained with a phosphor plate imaging system Digora Optime. Eight observers evaluated all the test images for carious lesion within the 90 proximal surfaces. With the histological examination serving as the reference standard, observer performances were evaluated by receiver operating characteristic (ROC) curves. The areas under the ROC curves were analyzed with two-way analysis of variance. No significant differences were found among the CBCT images and between CBCT and digital images when only proximal enamel caries was detected ($p=0.989$). With respect to the detection of proximal dentinal caries, significant difference was found between CBCT and digital images ($p<0.001$) but not among CBCT images. The spatial resolution did not have an impact on the detection accuracy of proximal caries in flat panel CBCT images. The flat panel CBCT images

scanned with high spatial resolution did not improve the detection accuracy of proximal enamel caries compared to digital intraoral images. CBCT images scanned with high spatial resolutions could not be used for proximal caries detection.

Keywords Digital intraoral radiography · Cone beam computerized tomography · Spatial resolution · Proximal caries · Detection accuracy

Introduction

It is widely accepted that radiography is a vital adjunct for the diagnosis of caries [1]. The rapid development of technology has given birth to various digital dental imaging modalities, including digital intraoral radiography and cone beam computerized tomography (CBCT) scanners. Meanwhile, the widespread use of fluorides has delayed cavitation and made carious lesions difficult to detect [2]. Therefore, it is imperative to identify the diagnostic accuracy of various imaging modalities for an appropriate treatment planning.

In the 1980s, digital imaging systems came into use in dentistry. Compared with traditional film technology, digital imaging systems have a number of advantages, such as adjustable images, avoidance of chemical processing, lower dose, less working time and convenient communication, etc. [3]. CBCT, introduced into the dental office in 1990s, uses a 2D X-ray detector and a cone- or pyramid-shaped X-ray beam to reconstruct isotropic, high-spatial-resolution, 3D images [4]. CBCT has created a revolution in maxillofacial imaging, facilitating the transition of dental diagnosis from 2D to 3D images and expanding the role of imaging from diagnosis to imaging guidance of

J.-G. Cheng · Z.-L. Zhang · Z.-Y. Zhang · X.-C. Ma · G. Li (✉)
Department of Oral and Maxillofacial Radiology,
Peking University School and Hospital of Stomatology,
#22 Zhongguancun Nandajie, Hai Dian District,
100081 Beijing, China
e-mail: kqgang@bjmu.edu.cn

X.-Y. Wang
Department of Operative Dentistry and Endodontics,
Peking University School and Hospital of Stomatology,
100081 Beijing, China

operative and surgical procedures by application of third-party software.

Nowadays, CBCT scanners are available that can give the user a choice between high and low spatial resolution settings when scanning a patient. In theory, the higher the number of the spatial resolution used for scanning, the smaller the radiographic details which can be observed in the resultant images [5]. However, one study indicates that the resolution did not have an impact on the detection of dental caries, neither proximal nor occlusal caries [6]. In this study, the NewTom 3 G was used to scan the extract human permanent teeth with three different resolution settings (FOV 12 in, 0.36 mm; FOV 9 in, 0.25 mm; FOV 6 in, 0.16 mm). The NewTom 3 G employed a detector using a configuration of scintillation screens, image intensifiers (II) and charge-coupled device (CCD) sensors.

Most of nowadays CBCT scanners, however, use a type of flat panel detector composed of Amorphous Silicon or CMOS (complementary metal–oxide semiconductor). The flat panel detector is believed to provide a greater dynamic range and greater performance than the II/CCD technology, which may create geometric distortion [4]. In the search of literature, we did not find one study exclusively evaluating the resolution impact on the proximal caries detection with a CBCT scanner using a flat panel detector. Therefore, the aims of the present study were: (1) to evaluate the detection accuracy of proximal caries in flat panel CBCT images scanned with different resolutions; (2) to assess whether the spatial resolutions have an impact on the detection accuracy of proximal caries in flat panel CBCT images; (3) to assess whether the detection accuracy of proximal caries can be improved by flat panel CBCT images scanned with high spatial resolution when compared with digital intraoral radiographs.

Materials and methods

Teeth

After preliminary visual examination, 45 non-restored human permanent premolars and molars were employed in the present study. Of the 90 proximal surfaces, six surfaces had obvious cavities. The clinical appearance of the remaining tooth surfaces ranged from sound to chalky or brown discolored after cleaning.

The teeth, four or five as a group, were mounted in 11 plaster blocks. When mounting, it was ensured that the prominent part of the proximal surfaces were in contact and at the same vertical level, simulating the normal anatomical position.

The 11 tooth blocks were then numbered and stored separately in 10% neutral buffered formalin solution.

Test images

CBCT images of the 11-block samples were acquired with two CBCT scanners: ProMax 3D (Planmeca Oy, Helsinki, Finland) and DCT Pro (VATECH, Co., Ltd., Yongin-Si, South Korea). Both scanners are flat panel type composed of CMOS. The ProMax 3D provided three resolution settings: low, normal and high resolutions, while the DCT Pro gave two resolution settings that were normal and high. To simulate soft tissue, a 20-mm-thick water phantom was placed around the blocks during exposure. The CBCT images were subsequently reconstructed with the proprietary software of each system.

Digital intraoral images of the 11-block samples were obtained using phosphor plate (Digora Optime digital imaging system; Soredex, Helsinki, Finland). The X-ray unit used was a Soredex MinRay with a focal spot size of 0.7 mm, 2-mm Al filtration and nominal tube potential selectable at either 60 or 70 kVcp. To mimic soft tissue, a 20-mm acrylic block was placed in front of the tooth block during exposure. The projection geometry was standardized by using a special designed holder. The proprietary phosphor plate was used to record the images. Digital images were obtained after exposure by immediately scanning the phosphor plates with the proprietary software Dfw v.2.5. The selected scanning resolution was 400 dpi. The raw data images were processed with the proprietary default processing algorithm and saved as 8-bit images. Figure 1 illustrates six images of the same tooth block.

The exposure specifications for taking the images are presented in Table 1.

Viewing

Eight postgraduate individuals viewed all test images that were categorized into six groups: (1) ProMax 3D low resolution images, (2) ProMax 3D normal resolution images, (3) ProMax 3D high resolution images, (4) DCT Pro normal resolution images, (5) DCT Pro high resolution images, and (6) phosphor plate images. All test images were displayed on a 22-in Dell TM E228WFP flat panel monitor (Dell, Round Rock, TX, USA) with a resolution of 1,680×1,050 pixels. The CBCT images were randomly run with the proprietary software and allowed to adjust the brightness and contrast by the observers at will and evaluated in axial, coronal, and sagittal planes with respect to proximal caries. The digital images were viewed randomly in the software package ACDseev.10.0 (ACD Systems International, British Columbia, Canada) at the display ratio of 1:1 and no extra adjustment was permitted. Before viewing, each observer was informed on the use of CBCT proprietary software and the definition of proximal caries. Viewing was conducted in a dimly lit room with no time

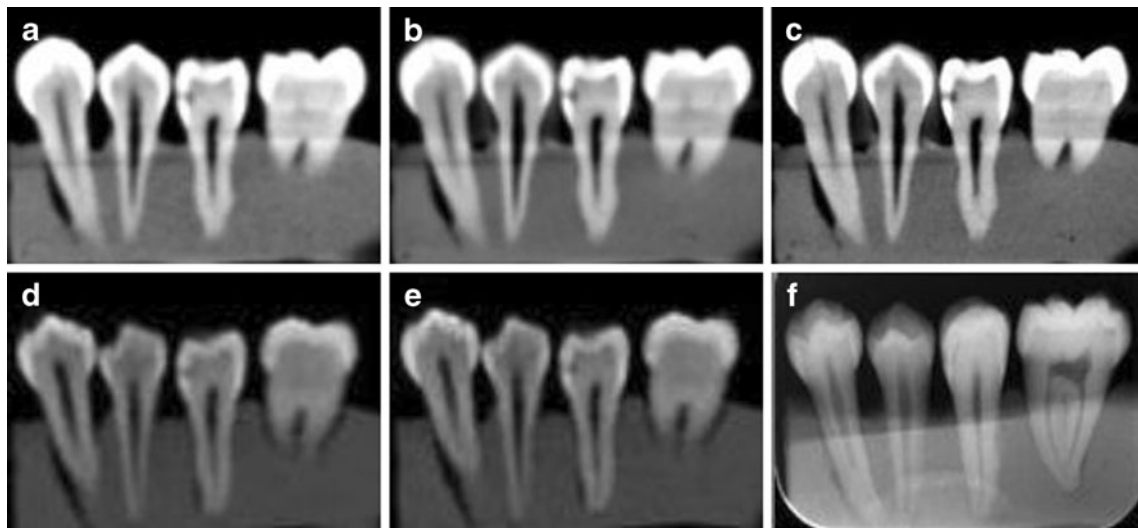


Fig. 1 Example images of the same tooth block scanned with ProMax 3D at low resolution (a), ProMax 3D at normal resolution (b), ProMax 3D at high resolution (c), DCT Pro at normal resolution (d), DCT Pro at high resolution (e) and phosphor plate (f)

restrictions. Each observer evaluated only one group of the test images at a time. There was at least 1-week interval between the adjacent evaluations of two groups. To investigate the intra-observer agreement, each observer reassessed all images 2 weeks later.

The observers used the following 5-point rank scale to record their level of confidence with regard to the absence or presence of proximal carious lesion: 1=definitely no caries, 2=probably no caries, 3=questionable, 4=probably caries, 5=definitely caries.

Histological validation

The tooth crowns of the 45 teeth were sectioned perpendicularly to the long axis of the tooth at a position a little bit lower than the enamel–cemental junction. After cleaning and drying, the 45 tooth crowns were individually embedded in polyacrylic resin. Each polyacrylic resin block was then sectioned (700 μm thick per slice) serially and mesiodistally in parallel with the long axis of the tooth crowns using Leica SP1600 saw microtome (Leica Microsystems GmbH, Wetzlar, Germany) with a 300-μm diamond saw blade.

The tooth slices were observed with a 16× magnifying stereomicroscope ZOOM-630E (Changfang Optical Instrument Ltd., Shanghai, China) by two investigators, who were calibrated before evaluation. Proximal carious lesion was defined as chalky white demineralization or brownish discoloration in the proximal surface. The following 6-point scale was used for histological stratification of the sites: 0=sound, 1=caries in the outer half of the enamel, 2=caries in the inner half of the enamel, 3=caries having reached but not crossed the enamel–dentinal junction (EDJ), 4=caries in the outer half of the dentine, 5=caries in the inner half of the dentine or into the pulp. The highest score from the various slices was considered as the true status of the assessed proximal surface. In case that two observers’ ratings were not the same, they performed a joint assessment to reach a consensus.

Data analysis

With the histological examination as reference standard, each observer’s performance was converted into a receiver operating characteristic (ROC) curve with SPSS v.16.0 for

Table 1 Specifications of the employed imaging systems for images

	(kV)	(mA)	Exposure time (s)	Detector	FOV (cm)	Voxel size (mm)	Slice thickness (mm)
ProMax 3D low resolution	84	6	3	CMOS	8×8	0.32	0.96
ProMax 3D normal resolution	84	12	12	CMOS	8×8	0.32	0.96
ProMax 3D high resolution	84	12	12	CMOS	8×8	0.16	0.48
DCT Pro normal resolution	90	7.5	15	CMOS	16×7	0.3	1
DCT Pro high resolution	90	7.5	24	CMOS	16×7	0.2	1
Phosphor plate	60	7	0.2	SPP	–	–	–

FOV field of view, SPP storage phosphor plate, CMOS complementary metal oxide semiconductor

Table 2 Areas under the receiver operating characteristic curves (A_z) obtained from each observer when detecting all proximal caries

Observer	ProMax 3D low resolution	ProMax 3D normal resolution	ProMax 3D high resolution	DCT Pro normal resolution	DCT Pro high resolution	Phosphor plate
1	0.625	0.610	0.625	0.609	0.625	0.594
2	0.610	0.634	0.632	0.610	0.632	0.594
3	0.652	0.646	0.663	0.635	0.586	0.576
4	0.632	0.612	0.625	0.610	0.619	0.598
5	0.650	0.660	0.646	0.628	0.638	0.630
6	0.591	0.618	0.612	0.595	0.593	0.579
7	0.561	0.632	0.611	0.704	0.649	0.607
8	0.663	0.622	0.659	0.625	0.659	0.564
Mean	0.623	0.629	0.634	0.627	0.625	0.593
SD	0.034	0.017	0.020	0.034	0.025	0.020

SD standard deviation

Windows (SPSS, Chicago, IL, USA). The maximum likelihood parameters were determined and the areas under the ROC curves (A_z values) were calculated. To probe into whether carious depth affects the observer’s performance, enamel caries and dentine caries were analyzed separately.

Two-way analysis of variance was used to analyze the A_z values for the differences among imaging modalities and observers. Intra-observer variation was analyzed with the paired t test. Differences were considered to be statistically significant when $p < 0.05$.

Results

Histological examination revealed that of the 90 proximal surfaces, 58(64.4%) were sound, 12(13.3%) had caries in the outer half of the enamel, 3(3.3%) had caries in the inner half of the enamel, three (3.3%) had caries having reached but not crossed the EDJ, 5(5.6%) had caries in the outer half of the dentine, nine (10.0%) had caries in the inner half of the dentine or into the pulp. Thus, a total of 32 proximal surfaces (35.6%) were considered to be positive for caries when performing the ROC analysis. Supposing that caries having reached but not crossed the EDJ were defined as

enamel caries, there would be 18 enamel caries (20.0%) and 14 dentine caries (15.6%).

Since there were no significant intra-observer difference (p values ranging from 0.071 to 0.718), ROC and two-way analysis of variance were based on the first readings. Table 2 demonstrates the individual and mean A_z values. There was significant difference in A_z values among the six groups of test images ($p=0.028$). Multiple comparisons of observer performances revealed that there was no significant difference among CBCT images, but there were significant differences between CBCT and digital images (Table 3). Meanwhile, no significant difference was found between observers ($p=0.134$).

When only enamel caries were taken into account, however, no significant difference was found in A_z values among the six groups of test images ($p=0.989$). Table 4 illustrates the multiple comparisons between observer performances obtained from each group of images. Figure 2 shows the ROC curves from the pooled observer performances. All six curves are overlapped together and close to the reference line.

With respect to dentine caries, there were no significant differences among the CBCT images, while significant differences were found between the CBCT and digital

Table 3 p Values when comparing observer performance of each modality for all caries

	ProMax 3D normal resolution	ProMax 3D high resolution	DCT Pro normal resolution	DCT Pro high resolution	Phosphor plate
ProMax 3D low resolution	0.615	0.372	0.747	0.864	0.019*
ProMax 3D normal resolution		0.694	0.856	0.740	0.005*
ProMax 3D high resolution			0.566	0.470	0.002*
DCT Pro normal resolution				0.880	0.009*
DCT Pro high resolution					0.013*

* $p < 0.05$, significant difference

Table 4 *p* Values when comparing observer performance of each modality for enamel caries

	ProMax 3D normal resolution	ProMax 3D high resolution	DCT Pro normal resolution	DCT Pro high resolution	Phosphor plate
ProMax 3D low resolution	0.853	0.892	0.732	0.847	0.643
ProMax 3D normal resolution		0.748	0.598	0.705	0.517
ProMax 3D high resolution			0.836	0.954	0.743
DCT Pro normal resolution				0.881	0.903
DCT Pro high resolution					0.786

images (Table 5). Figure 3 shows the ROC curves from the pooled observer performances. Generally, the ROC curves for CBCT images are higher than that for the digital images.

Discussion

An objective comparison of diagnostic accuracy of imaging systems requires a simultaneous evaluation of sensitivity and specificity [7]. ROC analysis, developed to evaluate the quality of signal detection by observers responding to stimuli in an environment of varying levels of noise, is a method that evaluates sensitivity and specificity simultaneously [8]. This method is a least-biased measure of diagnostic performance. ROC curve graphically presents the ratio of the sensitivity and false sensitivity responses as

a decision criterion is varied. The most common index to characterize an ROC curve is the A_z value, i.e., the area under the ROC curve. This value may vary from 0.5 to 1.0, in which 0.5 represents a random decision and 1.0 a perfect diagnostic justification [9]. ROC analysis yields valid measurements of observer performance in diagnostic tasks pertaining to the detection of carious lesions by radiography [10].

The CBCT scanners using flat panel detector were employed in the present study. However, the result that the spatial resolution did not have any impact on the detection accuracy of proximal caries is in line with that obtained from a previous study in which the CBCT scanner NewTom 3 G using a II/CCD detector was employed [6]. In addition, other studies show a similar result with respect to the effect of resolutions. In one study [11], the effect of voxel size on the detection of occlusal caries was assessed using the Iluma Ultra CBCT scanner. The results revealed that no significant differences were found between the ultra-resolution and the high- and low-resolution images. In the study [12] regarding the simulated external root resorption, the spatial resolution did not affect the sensitivity or specificity values of i-CAT in the diagnostic ability. For the study with respect to the detection of transverse root fractures [13], it was demonstrated that there was a significant difference between the CBCT images scanned with high and low spatial resolutions. In the present study, two CBCT scanners were employed. One was the ProMax 3D that could provide three resolution selections and the other was the DCT Pro which gave selections of high or normal resolutions. For the CBCT images scanned with the ProMax 3D at high, normal and low resolutions, the mean A_z values were 0.623, 0.629 and 0.634, respectively, while for the CBCT images scanned with the DCT Pro, the mean A_z value was 0.627 for the normal and 0.625 for the high resolution images. The results reveal that there were no significant differences among the CBCT images.

To further disclose the effect of spatial resolution on the CBCT images, the present study also compared the

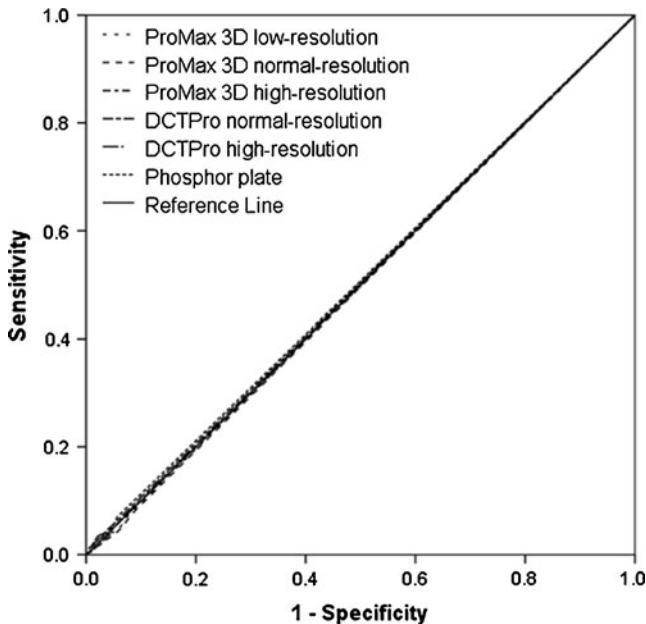


Fig. 2 Receiver operating characteristic (ROC) curves from the pooled observer performances for each imaging modality when only detecting proximal enamel caries

Table 5 *p* Values when comparing observer performance of each modality for dentine caries

	ProMax 3D normal resolution	ProMax 3D high resolution	DCT Pro normal resolution	DCT Pro high resolution	Phosphor plate
ProMax 3D low resolution	0.179	0.105	0.892	0.957	0.000**
ProMax 3D normal resolution		0.772	0.226	0.197	0.000**
ProMax 3D high resolution			0.136	0.117	0.000**
DCT Pro normal resolution				0.935	0.000**
DCT Pro high resolution					0.000**

** $p < 0.001$, significant difference

detection accuracy of proximal caries between the digital and CBCT images. It was revealed that when only caries confined in enamel were taken into consideration, no statistical significant differences were found between the CBCT and digital images no matter what spatial resolution used for scanning. This is in agreement with the previous study that the CBCT images acquired at different spatial resolutions performed equally well with digital images when evaluating health sound and superficial enamel occlusal caries [11].

When only the dentinal caries were evaluated, however, there were significant differences between the digital and CBCT images. In the study conducted by Young et al. [14], it was found that practicing dentists were able to improve their detection accuracy of proximal-surface caries extending into the dentine, using 3DX Accuitomo compared with CCD sensors.

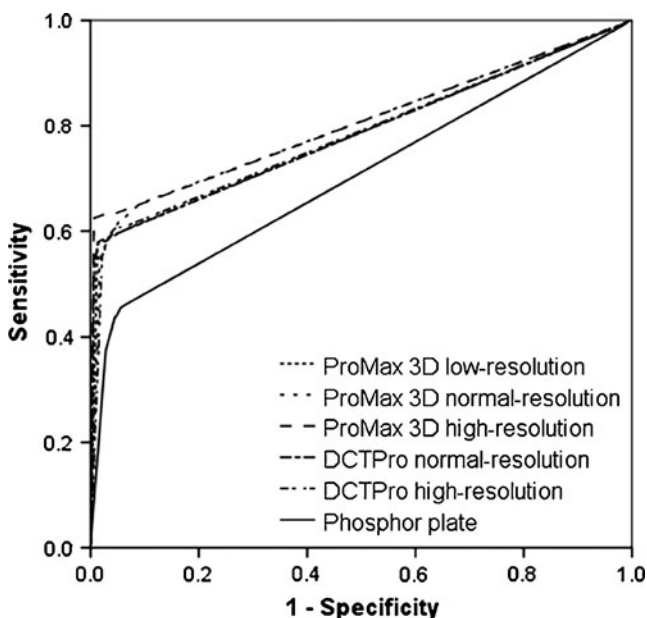


Fig. 3 Receiver operating characteristic (ROC) curves from the pooled observer performances for each imaging modality when only detecting proximal dentine caries

Despite of the possible advantages in diagnostic outcome of CBCT, it should be borne in mind that CBCT still results in higher radiation doses than conventional imaging examinations [15–18]. It is critical that the potential patient benefits from a radiographic examination be balanced against the risk of exposure to ionizing radiation. The principle of ALARA (As Low As Reasonably Achievable) is still fundamental for diagnostic radiology and CBCT procedures should be reserved for selected cases. Perhaps for caries detection, CBCT should be a secondary imaging modality to be used when conventional views provide equivocal results or when carious measurement is needed. Also, when a CBCT examination is indicated for other applications, e.g., implant site examination, it may be used as an adjunct for caries detection.

The main drawback of the present study is that the *in vitro* study simulated an ideal condition that excludes object movement, metallic restoration, tissue around teeth and other parameters that can complicate the diagnosis of caries. These factors, especially metallic restorations that produce beam hardening artifacts, may ultimately influence the image quality and thus the diagnostic accuracy when a real patient is diagnosed. Thus, for those teeth with metallic restorations the CBCT examination should be excluded.

In conclusion, the spatial resolution did not have an impact on the detection accuracy of the flat panel CBCT image for proximal caries. Since the radiation dose is increased when scanning a CBCT image with a high spatial resolution [19, 20], it is recommended that the low resolution that gives a low radiation dose be used for evaluating dentinal caries when necessary. The CBCT images should not be used for evaluating carious lesions confined in enamel.

Acknowledgements The study is supported by Capital Medicine Develop Research Foundation (No. 2009–3038). We express our sincere appreciations to all the observers who assessed the test images.

Conflict of interest The authors declare that they have no conflict of interest.

References

1. Stookey GK, Jackson RD, Zandona AG, Analoui M (1999) Dental caries diagnosis. *Dent Clin North Am* 43:665–677
2. Robinson C (2009) Fluoride and the caries lesion: interactions and mechanism of action. *Eur Arch Paediatr Dent* 10:136–140
3. Wenzel A (1998) Digital radiography and caries diagnosis. *Dentomaxillofac Radiol* 27:3–11
4. Scarfe WC, Farman AG (2008) What is cone-beam CT and how does it work. *Dent Clin North Am* 52:707–730
5. Ludlow JB, Mol A (2009) Digital imaging. In: White SC, Pharoah MJ (eds) *Oral radiology: principle and interpretation*, 6th edn. Mosby, Inc., Maryland Heights, pp 83–84
6. Haiter-Neto F, Wenzel A, Gottfredsen E (2008) Diagnostic accuracy of cone beam computed tomography scans compared with intraoral image modalities for detection of caries lesions. *Dentomaxillofac Radiol* 37:18–22
7. Berkey CS, Douglass CW, Valachovic RW, Chauncey HH, McNeil BJ (1990) Statistical methods for comparing dental diagnostic procedures. *Community Dent Oral Epidemiol* 18:169–176
8. Obuchowski NA (2003) Receiver operating characteristic curves and their use in radiology. *Radiology* 229:3–8
9. Sanderink GC, Huisken R, van der Stelt PF, Welander US, Stheeman SE (1994) Image quality of direct digital intraoral x-ray sensors in assessing root canal length. The RadioVisioGraphy, Visualix/VIXA, Sens-A-Ray, and Flash Dent systems compared with Ektaspeed films. *Oral Surg Oral Med Oral Pathol* 78:125–132
10. Verdonschot EH, Wenzel A, Bronkhorst EM (1993) Applicability of Receiver Operating Characteristic (ROC) analysis on discrete caries depth ratings. *Community Dent Oral Epidemiol* 21:269–272
11. Kamburoglu K, Murat S, Yuksel SP, Cebeci ARI, Paksoy CS (2010) Occlusal caries detection by using a cone-beam CT with different voxel resolutions and a digital intraoral sensor. *Oral Surg Oral Med Oral Pathol Oral Radiol Endod* 109:e63–e69
12. Liedke GS, Da Silveira HE, Da Silveira HL, Dutra V, De Figueiredo JA (2009) Influence of voxel size in the diagnostic ability of cone beam tomography to evaluate simulated external root resorption. *J Endod* 35:233–235
13. Wenzel A, Haiter-Neto F, Frydenberg M, Kirkevang LL (2009) Variable-resolution cone-beam computerized tomography with enhancement filtration compared with intraoral photostimulable phosphor radiography in detection of transverse root fractures in an in vitro model. *Oral Surg Oral Med Oral Pathol Oral Radiol Endod* 108:939–945
14. Young SM, Lee JT, Hodges RJ, Chang TL, Elashoff DA, White SC (2009) A comparative study of high-resolution cone beam computed tomography and charge-coupled device sensors for detecting caries. *Dentomaxillofac Radiol* 38:445–451
15. Danforth RA, Clark DE (2000) Effective dose from radiation absorbed during a panoramic examination with a new generation machine. *Oral Surg Oral Med Oral Pathol Oral Radiol Endod* 89:236–243
16. Ludlow JB, Davies-Ludlow LE, Brooks SL (2003) Dosimetry of two extraoral direct digital imaging devices: NewTom cone beam CT and Orthophos Plus DS panoramic unit. *Dentomaxillofac Radiol* 32:229–234
17. Ludlow JB, Davies-Ludlow LE, Brooks SL, Howerton WB (2006) Dosimetry of 3 CBCT devices for oral and maxillofacial radiology: CB Mercuray, NewTom 3 G and i-CAT. *Dentomaxillofac Radiol* 35:219–226
18. Ludlow JB, Davies-Ludlow LE, White SC (2008) Patient risk related to common dental radiographic examinations: the impact of 2007 International Commission on Radiological Protection recommendations regarding dose calculation. *J Am Dent Assoc* 139:1237–1243
19. Pauwels R, Beinsberger J, Collaert B et al (2010) Effective dose range for dental cone beam computed tomography scanners. *Eur J Radiol*. doi:10.1016/j.ejrad.2010.11.028
20. Qu XM, Li G, Ludlow JB, Zhang ZY, Ma XC (2010) Effective radiation dose of ProMax 3D cone-beam computerized tomography scanner with different protocols. *Oral Surg Oral Med Oral Pathol Oral Radiol and Endod* 110:770–776